Journal of Molecular Structure 1234 (2021) 130168

Contents lists available at ScienceDirect

Journal of Molecular Structure

journal homepage: www.elsevier.com/locate/molstr

Structure based design, synthesis and evaluation of new thienopyrimidine derivatives as anti-bacterial agents

Satyaveni Malasala[a], Anusha Polomoni[b], Md. Naiyaz Ahmad[c,d], Manjulika Shukla[c], Grace Kaul[c,d], Arunav Dasgupta[c,d], Sidharth Chopra[c,d,*], Srinivas Nanduri[a,*]

[a] Department of Medicinal Chemistry, National Institute of Pharmaceutical Education and Research (NIPER), Hyderabad 500 037, Telangana, India
[b] Department of Process Chemistry, National Institute of Pharmaceutical Education and Research (NIPER), Hyderabad 500 037, Telangana, India
[c] Division of Microbiology, CSIR-Central Drug Research Institute, Sitapur Road, Sector 10, Janakipuram Extension, Lucknow-226031, Uttar Pradesh, India
[d] AcSIR, Ghaziabad, Sector 19, Kamla Nehru Nagar, Ghaziabad-201002, Uttar Pradesh, India

ARTICLE INFO

Article history:
Received 14 November 2020
Revised 13 February 2021
Accepted 16 February 2021
Available online 24 February 2021

Keywords:
Thienopyrimidine
Structure-based design
Anti-bacterial agents

ABSTRACT

TrmD, tRNA-(N^1G37) methyltransferase, a member of SpoU-TrmD (SPOUT) RNA methyltransferase family, is one of the key enzymes responsible for the growth of *Staphylococcus aureus, Pseudomonas aeruginosa, Mycobacterium tuberculosis* (Mtb) and *Mycobacterium abscessus* (Mab). A number of TrmD inhibitors including thienopyrimidines and fused thienopyrimidines are reported as potent anti-bacterial and anti-mycobacterial agents. In the current study, a library of ~200 structurally diverse thienopyrimidines were designed and subjected to preliminary *in silico* studies. 22 of the compounds were selected, synthesized and were evaluated for their inhibitory activities against a panel of pathogens consisting *E. coli, S. aureus, K. pneuminiae, A. baumannii* and *P. aeruginosa* and *M. tuberculosis* (ATCC 27294). Among the tested compounds, **13b, 18a-e** were found to inhibit *M. tuberculosis* (ATCC 27294) with the MIC of 16-32 μg/mL. The compound **18f** was found to be selective against *S. aureus* with the MIC of 4 μg/mL and moderate activity against *M. tuberculosis*. The selected compounds were further subjected to docking, 3D-QSAR and ADME/T studies to understand the mechanism of action and also their physico chemical profile.

1. Introduction

TrmD, tRNA-(N^1G37) methyltransferase, is one of the members in the SpoU-TrmD (SPOUT) RNA methyltransferase family which transfers methyl group from *S*-adenosyl methionine (SAM) to the N^1 position of guanosine 37 in bacterial tRNA [1,2]. TrmD has been shown to be crucial for the growth of *Staphylococcus aureus, Pseudomonas aeruginosa, Mycobacterium tuberculosis* (Mtb) and *Mycobacterium abscessus* (Mab) [3,4]. Hill et al. in 2013 [5] reported the design and synthesis of thienopyrimidinone based TrmD inhibitors binding to *S*-Adenosyl-methionine (SAM)-binding pocket using fragment-based screening approach (Fig. 1. Compound **A**). Whitehouse et al. [6] reported Indole and Pyrazole based compounds **B-D** (Fig. 1) as potent inhibitors of Mab TrmD. Zhong et al. [7] identified compound **E** from a radioactivity-free, bioluminescence-based high throughput screen (HTS) of 116350 compounds from structurally diverse small-molecule libraries as potent inhibitor of *Pseudomonas aeruginosa* TrmD (Pa TrmD) (Fig. 1).

Thienopyrimidine ring is considered as a bio isostere of quinazoline ring. In recent years, thienopyrimidines and fused thienopyrimidines have attracted the attention of medicinal chemists owing to their promising antimicrobial [8], antiviral [9], anti-inflammatory [10], antidiabetic [11], antioxidant [12] and anxiolytic [13] activities. Hafez et al. [14] reported several heterocyclic substituents directly linked to thienopyrimidine nucleus at C-2. Further, various thieno [2,3-d] pyrimidines derived from 2-thioxothienopyrimidine were prepared as potent anti-HIV and antimicrobial agents (Fig. 2. Compound **I**). Abbas et al. [15] reported 2,3 and 3,4-disubstituted tetrahydrobenzo[4,5]thieno[2,3-d]pyrimidines as potent anti-cancer and anti-bacterial agents amongst which 3-acridin-3-yl derivatives exhibited notable activity against the tested bacterial strains (Fig. 2. Compound **II**). Li et al. [16] reported optimisation of compound **III,** an antitubercular hit compound against CD117 using chemocentric approach (Fig. 2).

In the current study, a library of ~200 structurally diverse thienopyrimidines were designed as potential inhibitors of TrmD

* Corresponding authors:
E-mail addresses: skchopra007@gmail.com (S. Chopra), nandurisrini92@gmail.com (S. Nanduri).

https://doi.org/10.1016/j.molstruc.2021.130168
0022-2860/

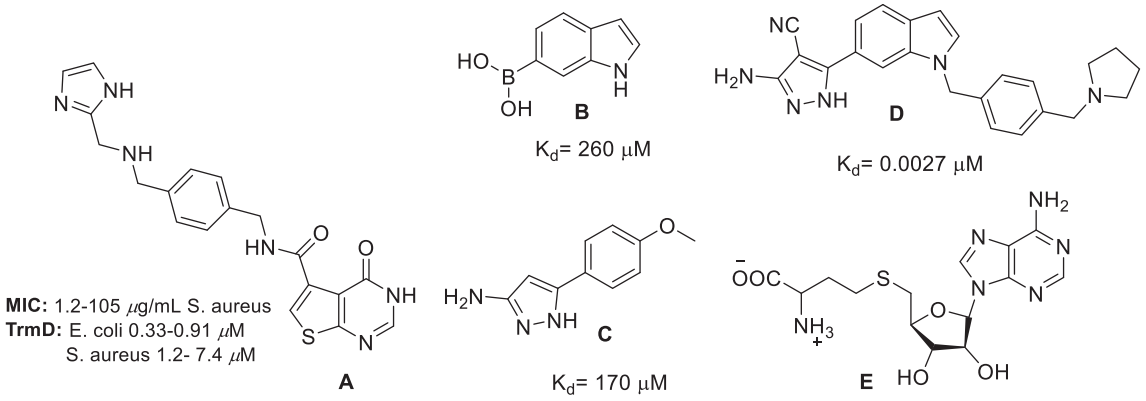

Fig. 1. Reported TrmD inhibitors.

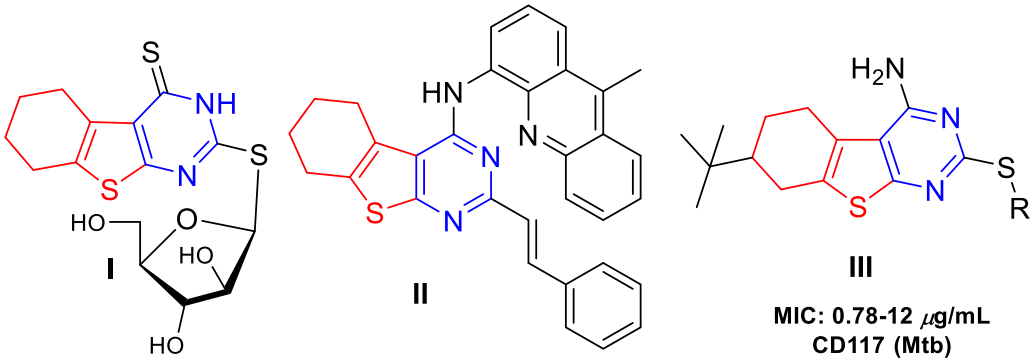

Fig. 2. Reported thienopyrimidines as anti-bacterial agents.

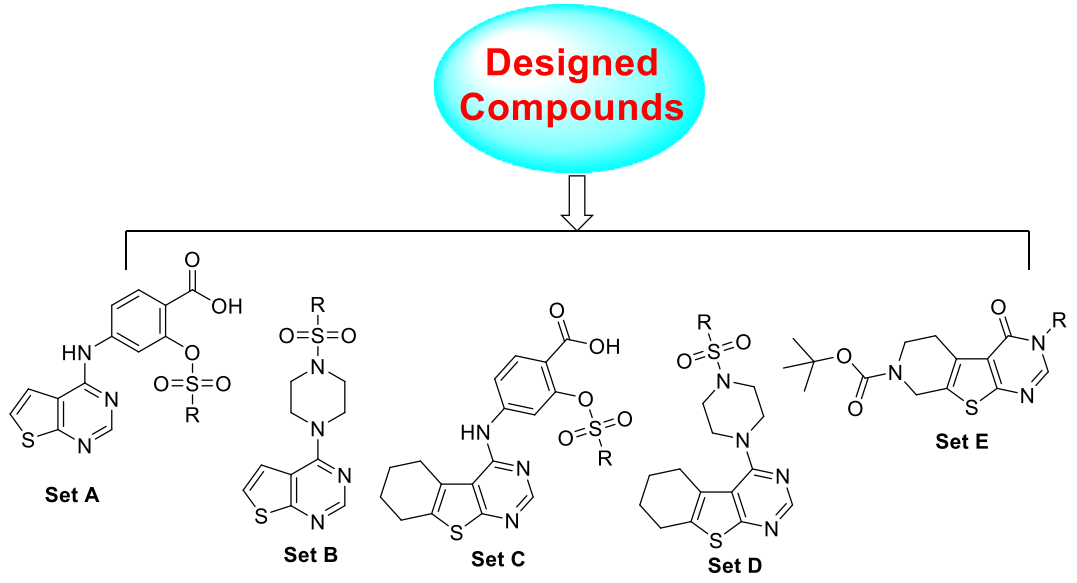

Fig. 3. Designed thienopyrimidine derivatives.

Fig. 3. Five sets of these thienopyrimidine containing molecules were selected and *in-silico* studies were performed (supporting information). Three of the series were found to fit well in the binding pocket and exhibit the necessary protein-ligand interactions. Molecular modelling studies helped us to understand the binding site and their interactions at the active pocket. Based on these studies and synthetic feasibility, 22 of the selected thienopyrimidines were synthesized Fig. 4.

2. Results and discussion

2.1. Molecular modelling

2.1.1. Selection of the therapeutic target

Among the many biological processes, modifications in the tRNA are critical for the bacterial survival which makes TrmD as one of the potential therapeutic targets for the development

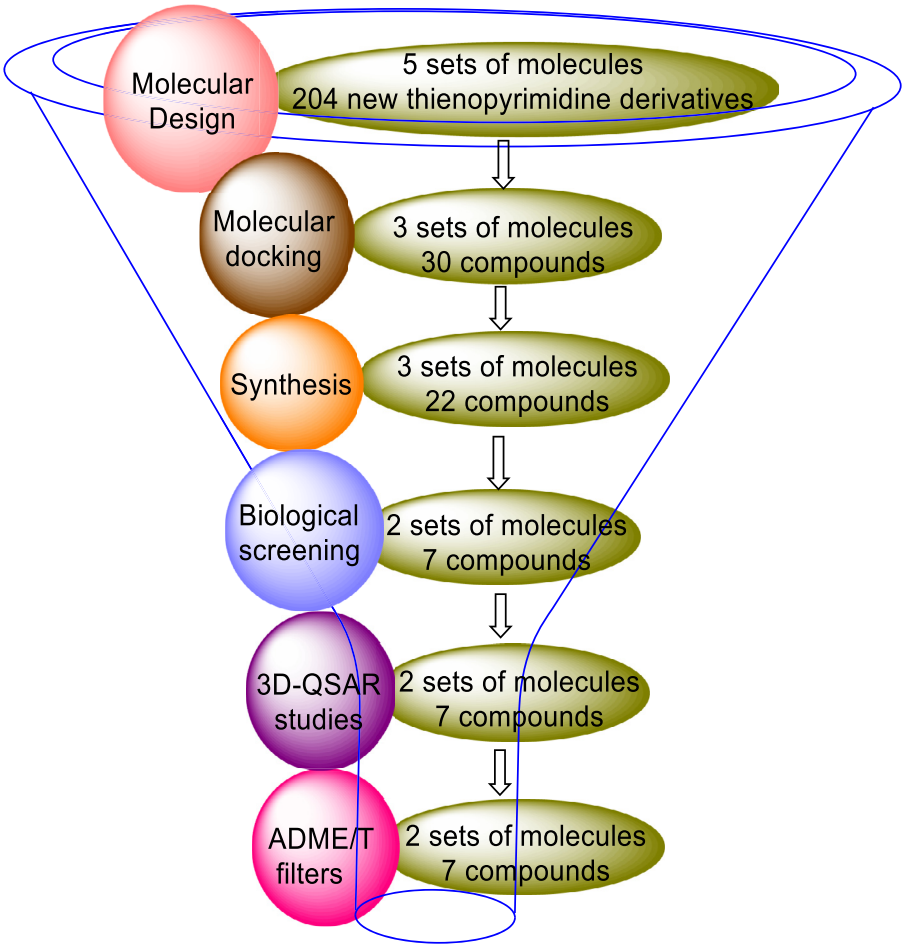

Fig. 4. Workflow for thienopyrimidine derivatives.

of new antibacterial agents. In the current study, we carried out structure-based design of new thienopyrimidine derivatives as potential TrmD inhibitors. The crystal structures of TrmD from *P. aeruginosa* and *M. tuberculosis* are utilized for this purpose.

2.1.2. Protein structure preparation

The coordinates for the TrmD receptor were downloaded from the RCSB protein data bank (PDB ID: 1UAK). The protein structure was processed using the Protein Preparation Wizard (PPW) and its integrity was checked and adjusted by adding the missing residues by employing Prime module of Schrödinger suite. The water molecules and all other heteroatoms were removed from the protein crystal structure. The H-bond network was optimized and the overlapping hydrogens were fixed under the refine tab of PPW. The most likely positions of thiol and hydroxyl hydrogen atoms, protonation states and tautomer of various amino acid residues were selected by the procedure captured from the protein assignment (Schrödinger). The pH range was set to 7.0 and the protein was minimized by applying OPLS_2005 force field. Finally, restrained minimization was performed until the average root mean square deviation (RMSD) of the non-hydrogen atoms converged to 0.30^{o}A.

2.2. Ligand preparation

A total of 204 molecules were constructed on Chemdraw11.0 version and imported to Maestro as SDF format files and optimized using OPLS_2005 force field in LigPrep module of Schrödinger software 2017-1. All the possible conformations and ionization states were calculated for ligands at a pH of 7.4 using Ionizer. The tautomeric states were generated for chemical groups with possible tautomerism.

2.3. Molecular docking

The newly designed molecules were docked against TrmD crystal structure to determine their inhibitory potential. Molecular docking studies were performed by using GLIDE (Grid-based Ligand Docking with Energetics) docking module of Schrödinger. The prepared ligands were imported from the Ligprep docked into the generated receptor grid using Glide SP docking precision. The obtained results suggested the favourable interactions between the ligands and the protein. Van-der Waals scaling factor and partial charge cut-off was selected to be 0.80 and 0.15, respectively for ligand atoms. The interactions of each complex were interpreted and the 3D poses of the molecular interactions were collected using Schrödinger suite 2017-1.

2.4. ADME/T studies

ADME/T properties of the synthesized compounds were calculated using Qikprop program (Qikprop, version 6.5, Schrödinger, LLC, New York, NY, 2014). ADME/T studies, which help in predicting both physico-chemical significant descriptors and pharmacokinetically important properties of the molecules.

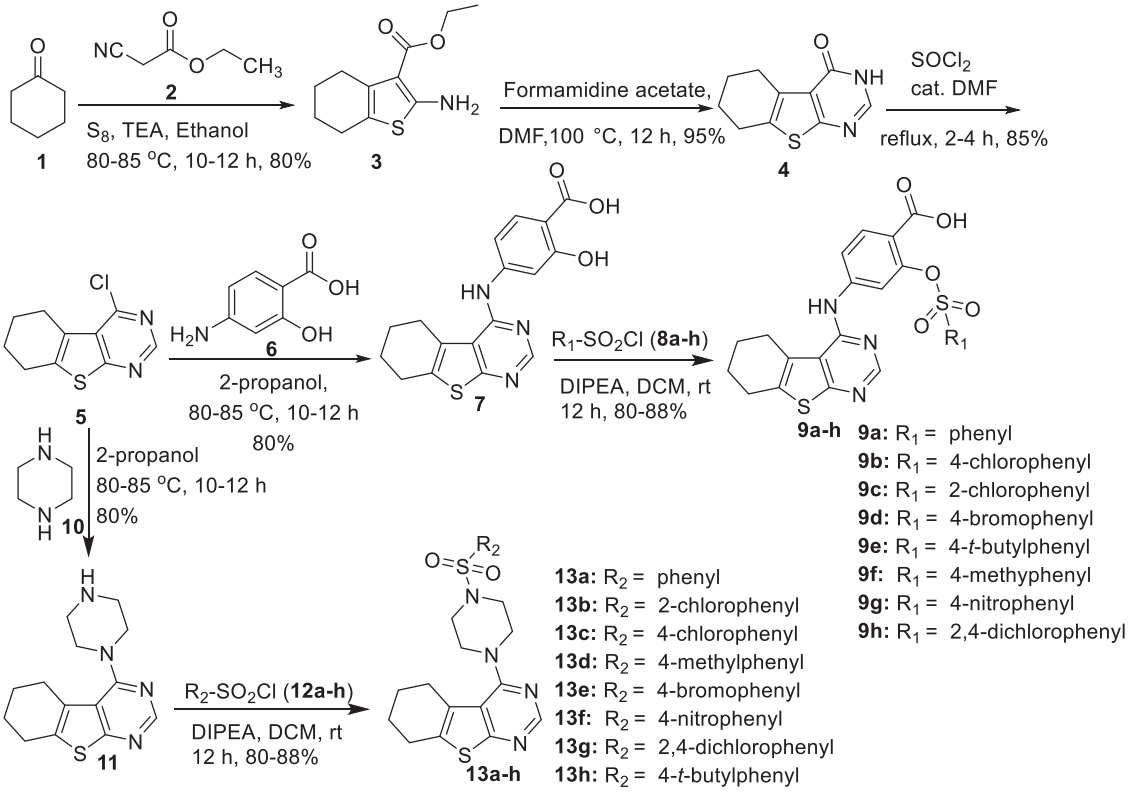

Scheme 1. Synthesis of 5,6,7,8-tetrahydrobenzo[4,5]thieno[2,3-d]pyrimidine sulphonyl esters **9a-h** and sulphonamides **13a-h**.

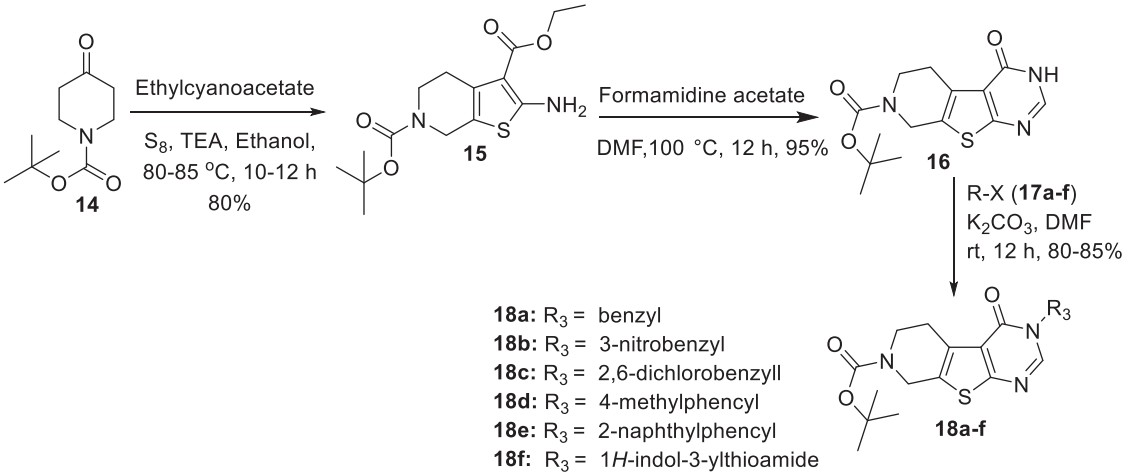

Scheme 2. Synthesis of tert-butyl 4-oxo-3,5,6,8-tetrahydropyrido[4′,3′:4,5]thieno[2,3-d]pyrimidine-7(4H)-carboxylate derivatives **18a-f**.

2.5. 3D-QSAR studies

The 3D-QSAR explains the key molecular interactions which are required for the biological activity and serves as a predictive tool. Construction of all the target compounds, structural optimization and 3D-QSAR modelling were performed on maestro software of Schrödinger.

2.6. Chemistry

A series of new thienopyrimidine derivatives were synthesized as described in Schemes 1 and 2. Cyclohexanone **1** or *N*-Boc-piperidone **13** were reacted with ethylcyanoacetate **2** to prepare the substituted thiophene intermediates **3** &**14** through the Gewald reaction. Further cyclisation with the formamidine acetate gave the substituted thienopyrimidine intermediates **4** and **15**. These intermediate **4** was treated with thionyl chloride and catalytic amount of *N, N*-dimethylformide to provide 4-chloro-5,6,7,8-tetrahydrobenzo [4,5] thieno[2,3-d] pyrimidine derivative **5**. The chlorinated derivative **5** undergoes nucleophilic substitution with *p*-amino benzoic acid **6** and piperazine **10** to obtain 2-hydroxy-4-(5,6,7,8-tetrahydrobenzo[4,5]thieno[2,3-d]pyrimidin-4-yl)amino) benzoic acid **7** and 4-(piperazin-1-yl)-5,6,7,8-tetrahydrobenzo[4,5]thieno[2,3-d]pyrimidine **11** which were treated with different substituted aryl sulphonyl chlorides using triethylamine as a base to give the corresponding sulphonyl esters **9a-h** and sulphonamide derivatives **13a-h** in good to moderate yields. The intermediate **16** was subjected to *N*-alkylation with different benzyl halides **17a-f** to obtain the corresponding products **18a-f** in good to moderate yields.

Table 1
MIC (μg/mL) values of *p*-amino salicylic acid/piperazine linked thienopyrimidine derivatives **9a-h, 13a-h & 18a-f.**

Sample Code	*S. aureus* ATCC 29213	*E. coli* ATCC 25922	*K. pneumoniae* BAA 1705	*A. baumannii* BAA 1605	*P. aeruginosa* ATCC 27853	Mtb H37Rv ATCC 27294	cLogP
9a	>64	>64	>64	>64	>64	>64	4.06
9b	>64	>64	>64	>64	>64	>64	4.61
9c	>64	>64	>64	>64	>64	>64	4.59
9d	>64	>64	>64	>64	>64	>64	4.68
9e	>64	>64	>64	>64	>64	>64	5.3
9f	>64	>64	>64	>64	>64	>64	4.37
9g	>64	>64	>64	>64	>64	>64	3.4
9h	>64	>64	>64	>64	>64	>64	4.96
13a	>64	>64	>64	>64	>64	>64	3.27
13b	>64	>64	>64	>64	>64	**16**	3.78
13c	>64	>64	>64	>64	>64	>64	3.76
13d	>64	>64	>64	>64	>64	>64	3.61
13e	>64	>64	>64	>64	>64	>64	3.88
13f	>64	>64	>64	>64	>64	>64	2.53
13g	>64	>64	>64	>64	>64	>64	4.28
13h	>64	>64	>64	>64	>64	>64	4.47
18a	>64	>64	>64	>64	>64	**16**	3.45
18b	>64	>64	>64	>64	>64	**32**	2.71
18c	>64	>64	>64	>64	>64	**32**	4.51
18d	>64	>64	>64	>64	>64	**16**	3.58
18e	>64	>64	>64	>64	>64	**32**	4.1
18f	**4**	>64	>64	>64	>64	**32**	3.75

2.7. In-vitro *anti-bacterial evaluation*

The newly synthesized thienopyrimidine derivatives were subjected to antibiotic susceptibility testing against a pathogen panel consisting of *E. coli, S. aureus, K. pneuminiae, A. baumannii* and *P. aeruginosa*. The minimum inhibitory concentrations (MICs) against the above pathogen panel were determined by using broth microdilution assay. In addition, the synthesized compounds were also evaluated against *M. tuberculosis* (ATCC 27294). The results are tabulated in Table 1.

The compounds **9a-h** derivatives were synthesized with *p*-amino salicylic acid as the linker and by varying different R_1 groups in the sulphonyl ester moiety. Thus, the compounds **9a** with phenyl group, **9b** with 4-chloro-phenyl, **9c** with 2-chlorophenyl, **9d** with 4-bromophenyl, **9e** with 4-*t*-butylphenyl, **9f** with 4-toluyl, **9g** with 4-nitrophenyl and **9h** with 2,4-dichlorophenyl moieties were synthesized. When tested, the compounds **9a-h** were found to be devoid of inhibitory activity against the bacterial pathogen panel and also *M. tuberculosis*. Next, we changed the linker to piperazine and synthesized different *N*-sulphonamide derivatives **13a-h** by changing R_2. Thus, compounds **13a** with phenyl group, **13b** with 2-chloro-phenyl, **13c** with 4-chlorophenyl, **13d** with 4-toulyl, **13e** with 4-bromophenyl, **13f** with 4-nitrophenyl, **13g** with 2,4-dichlorophenyl and **13h** with 4-t-butylphenyl moieties were synthesized and tested against the bacterial pathogen panel and *M. tuberculosis* (ATCC 27294). Among the tested compounds **13b** showed good and specific anti-mycobacterial activity with 16 μg/mL.

Subsequently, we changed the tetrahydrocyclic core with *N*-boc-piperidine and synthesized compounds **18a-f** with different R_3 groups. R_3 groups were varied with various benzyl groups such as unsubstituted benzyl **18a**, 3-nitro benzyl **18b** and 2,6-dichloro benzyl **18c**. Compounds **18d** and **18e** were synthesized with 4-methyl phenacyl and 2-napthyl phenacyl groups respectively. The compounds **18a–e** were found to possess inhibitory activity against *M. tuberculosis* with 16-64 μg/mL. When the R_3-group was changed to indole thioamide moiety as in **18f,** the compound showed selective inhibitory activity against *S. aureus* with an MIC value of 4 μg/mL and possess the moderate inhibitory activity against *M. tuberculosis* with 32 μg/mL.

Table 2
Cytotoxicity profile against Vero cells and Selectivity Index (SI).

Sample code	MIC (*S. aureus*) (μg/mL)	CC_{50}	SI
18f	4	50	>12.5

The compound **18f** was further subjected to cytotoxicity assay against Vero cells using MTT assay. The CC_{50} (50% cytotoxic concentration) was defined as the reduction of cell viability to 50% by compound. Doxorubicin and Levofloxacin were used as a reference standard and each experiment was performed in triplicate. The cytotoxicity data demonstrates that compound **18f** was nontoxic to Vero cells (CC_{50} = 50 μg/mL) and displayed favourable selectivity index Table 2.

Based on the above screening results, we identified compounds **13b, 18a-e** to possess inhibitory activity against *M. tuberculosis* and compound **18f** to possess selective inhibitory activity against *S. aureus*. As structurally related molecules are reported to be inhibitors of TrmD, the newly synthesized molecules were subjected to various *in-silico* studies against TrmD to further understand their mechanism of action. The compounds were subjected to docking, 3D-QSAR and ADME/T studies.

2.8. In-silico *studies*

As structurally related molecules are reported to exhibit inhibitory activity against bacterial t-RNA-(N1G37) Methyltransferase (TrmD), the newly synthesized molecules were docked against bacterial t-RNA-(N1G37) Methyltransferase (TrmD) crystal structure to determine their inhibitory potential. The 3D crystal co-ordinates of bacterial TrmD were retrieved from the protein data bank (PDB ID: 1UAK). Molecular docking studies were performed for the selected bio-active molecules (Fig. 5).

2.8.1. Prime MM/GBSA binding energy calculations

In our studies, we observed that all the active compounds have shown greater binding energies compared to the co-crystal binding energy, calculated by using MM/GBSA tool. The objective of MM/GBSA and docking studies is to explain the potential of the synthesized compounds as inhibitors of TrmD. In our studies, we

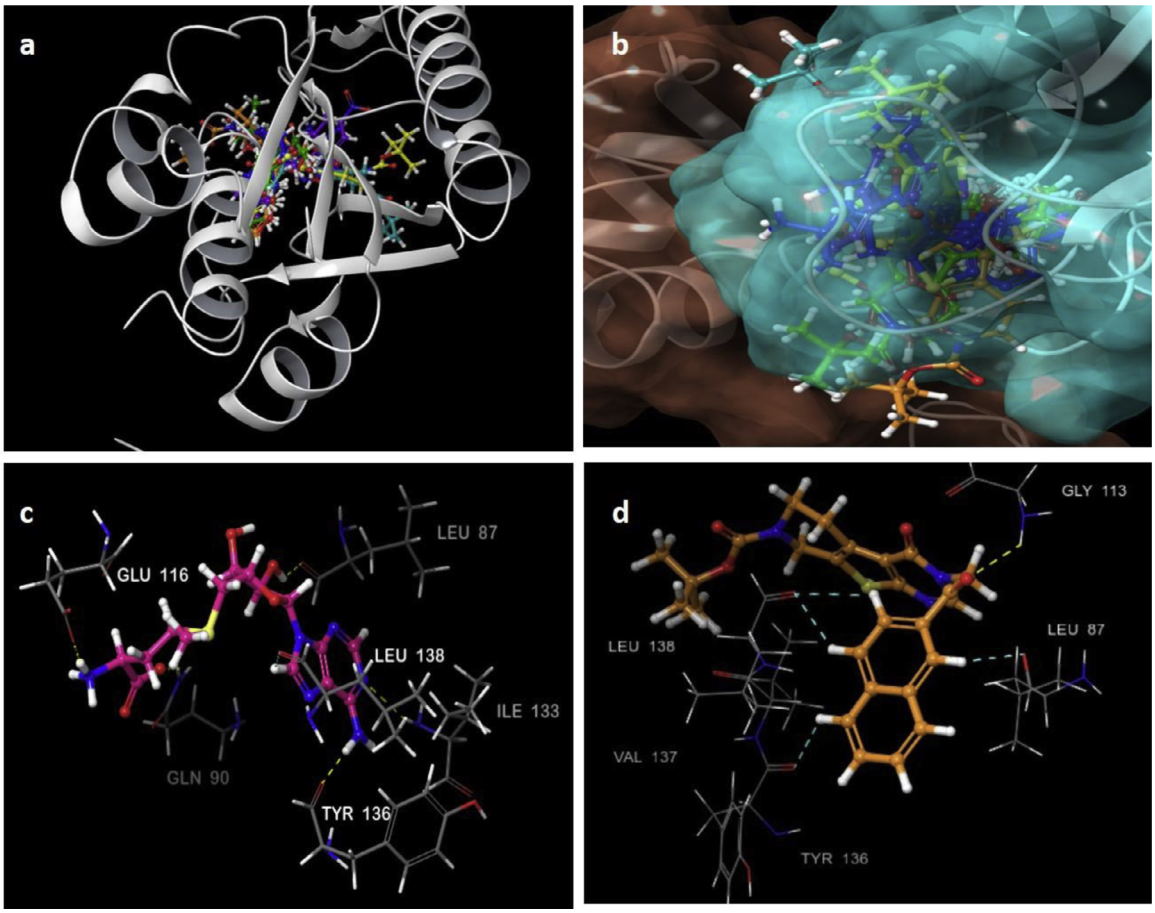

Fig. 5. **(a)** Protein overview with the binding pose of the molecules (ball and stick representation) and ligand interactions in the binding pocket of TrmD (PDB ID: 1UAK). The gold colour lines represent hydrogen bond interactions, the cyan colour lines imply the aromatic hydrogen bond interactions. (**b)** Super imposition of **13b, 18a-e** and **18f** at the binding pocket of TrmD (PDB ID: 1UAK). (**c)** Super imposition of **18f** (ball and stick representation-purple colour) at the binding pocket. (**d**) Super imposition of **co-crystal** (ball and stick representation-orange colour) at the binding pocket.

Table 3
Binding energy and ligand interactions of docked molecules (**13b** and **18a-f**).

S. No	Ligand id	Binding Energy (Kcal/mol)	Ligand-Protein interactions	
			H-Bond	Hydrophobic
	13b	-32.72	-	Tyr86, Leu87, Pro89, Tyr115, Trp131, Ile133, Tyr136, Val137, Leu138, Pro144
	18a	-48.62	-	Leu67, Tyr86, Leu87, Pro89, Tyr115, Ile123, Trp131, Ile133, Tyr136, Val137, Leu138, Pro144
	18b	-34.99	-	Tyr86, Leu87, Pro89, Cys112, Tyr115, Trp131, Tyr136, Val137, Leu138, Pro144
	18c	-44.21	-	Tyr86, Leu87, Pro89, Cys112, Tyr115, Tyr136, Val137, Leu138, Pro144
	18d	-54.82	Gly113	Pro58, Tyr86, Leu87, Pro89, Tyr115, Ile133, Tyr136, Val137, Leu138, Pro144
	18e	-57.80	Gly113	Tyr86, Leu87, Pro89, Cys112, Tyr115, Ile123, Trp131, Ile133, Tyr136, Val137, Leu138, Pro144
	18f	-47.92	Leu138	Pro58, Tyr86, Leu87, Pro89, Tyr115, Ile118, Trp131, Ile133, Tyr136, Val137, Leu138, Pro144
	Co-crystal	-60.88	Leu87, Gln90, Glu116,Ile13,Tyr136	Tyr86, Leu87, Pro89, Tyr115, Trp131, Ile133, Tyr136, Val137, Leu138, Pro144

observed that the synthesized compounds have shown good ligand interactions and binding energies at the binding pocket of TrmD as shown in Table 3. The active molecules displayed binding energies ranging from -32.72 to -57.80 kcal/mol in comparison to the co-crystal binding energy -60.80 kcal/mol. Finally, some of the identified ligands confirmed better binding energy compared to the co-crystal, suggesting that the synthesized compounds fit well for inhibiting TrmD Table 3.

2.9. 3D-QSAR studies

To explore the SARs of thienopyrimidines, the *in vitro* anti-bacterial and anti-mycobacterial activity data was selected to explains the three-dimensional quantitative structure activity relationship (3D-QSAR) models. Following the comprehensive procedure manual described in the literature, the MIC values of all derivatives against anti-bacterial and anti-mycobacterial were picked and transformed to predicted values.

2.9.1. Field and atom-based 3D-QSAR analysis

The accurate PLS statistics outcomes of the Field and atom-based 3D-QSAR models were disclosed in Table 4. The experimental and the predicted activity values of the target compounds against bacterial and tuberculosis are depicted in Table 5. The PLS study elucidates the predictive aptitude and the self-consistence of the model in which, the cross-validation correlation coefficient (q^2) and correlation coefficient (r^2) are two essential measures to figure out the strength of PLS analysis. The cross-validation correlation coefficient of more than 0.3 will be advised statistically as the chance of noticeable correlation being <95%. The q^2 and r^2 of

Table 4
PLS statistics of Field and Atom based 3D-QSAR models.

	q^2 [a]	r^2 [c]	SE [d]	F [e]	Fraction[f]				
					Steric	Electrostatic	Hydrophobic	H-Donor	H-Acceptor
Field 3D-QSAR	0.176	0.54	14.51	10.7	0.532	0.119	0.193	0.02	0.131
Atom 3D-QSAR (bacterial)	0.000	0.000	6.65	65.0	-	-	0.671	0.007	-
Atom 3D-QSAR (Tb)	0.134	0.373	16.50	51.0	-	-	0.671	0.005	-

[a]Cross-validated correlation coefficient.
[b]Optimum number of components obtained from cross-validated PLS analysis and same used in final non-cross-validated analysis.
[c]Non-cross-validated correlation coefficient.
[d]Standard error of estimate.
[e]F-test value. [f] Field contributions.

Table 5
Experimental and predicted activity values against *S. aureus* and H37Rv (MTb) of compounds for Field and Atom-based 3D-QSAR models.

Entry	Activity		Field (tb)		Atom (Bacterial)		Atom (tb)	
	*S. aureus*MIC(μg/mL)	Mtb, H37RvMIC(μg/mL)	Predicted activity	Prediction error	Predicted activity	Prediction error	Predicted activity	Prediction error
9a	>64	>64	>68.785	>4.785	>64.145	>-0.145	>70.193	>6.193
9b	>64	>64	>69.202	>5.207	>63.614	>-0.385	>70.531	>-6.531
9c	>64	>64	>59.414	>-4.585	>57.578	>-6.421	>54.726	>9.273
9d	>64	>64	>69.241	>5.241	>63.889	>-0.110	>70.563	>-6.563
9e	>64	>64	>66.394	>2.394	>55.860	>-8.139	>66.862	>-2.862
9f	>64	>64	>66.160	>2.160	>60.226	>-3.773	>64.319	>-0.319
9g	>64	>64	>66.215	>2.215	>61.725	>-2.274	>63.659	>0.340
9h	>64	>64	>59.583	>-4.416	>57.796	>-6.203	>54.742	>9.257
13a	>64	>64	>46.423	>-17.576	>68.644	>4.644	>48.755	>15.244
13b	>64	**16**	46.046	30.046	>68.682	>4.682	46.260	>30.260
13c	>64	>64	>46.715	>-17.284	>68.397	>4.397	>49.737	>-14.262
13d	>64	>64	>47.065	>-16.934	>68.872	>4.872	>49.715	>-14.
13e	>64	>64	>46.800	>-17.199	>68.359	>4.359	>49.769	>-14230
13f	>64	>64	>47.274	>-16.725	>69.033	>5.033	>48.916	>-15.083
13g	>64	>64	>46.188	>-17.811	>68.976	>4.976	>46.824	>-17.175
13h	>64	>64	>48.232	>-15.767	>68.122	>4.122	>48.047	>-15.952
18a	>64	**16**	44.059	28.059	>55.794	>-8.205	51.942	35.942
18b	>64	**32**	34.949	2.949	>49.663	>-14.336	44.876	12.876
18c	>64	**32**	32.600	0.600	>58.185	>-5.814	49.994	17.994
18d	>64	**16**	25.069	9.069	>48.125	>-15.874	31.164	15.164
18e	>64	**32**	33.410	1.410	>48.552	>-15.447	49.351	-14.648
18f	**4**	**32**	32.010	0.010	10.637	6.637	46.225	-14.225

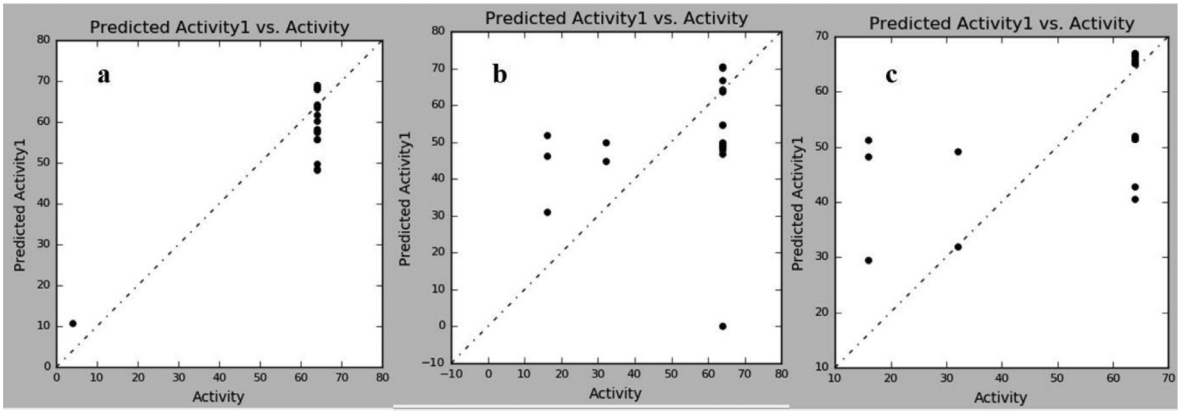

Fig. 6. Experimental activity *vs* predicted activity values for the synthesized compounds obtained by using Atom (Fig. 6**a**-Bacterial and Fig. 6**b**-tb) Field (Fig. 6**c**-tb) and based models.

the field-based model against tuberculosis were 0.176 and 0.54 and the atom-based model against bacterial q^2 and r^2 were 0.000, because the synthesized compounds did not show positive sign towards bacterial except **18f** so it is difficult to generate the corresponding q^2 and r^2 values. Atom based model against tuberculosis q^2 and r^2 were 0.134 and 0.373 and tabulated in Table 4 . The ideal sum of components used to produce field and atom-based models were in the acceptable range. The Fisher test results of models were found to be 10.7, 128.3 and 51.0 respectively. Furthermore, the predicted standard errors of the field and atom-based models were found to be 14.51, 4.885 and 8.363 respectively. The obtained results suggested that the field and atom-based models constructed were consistent and supportable modification of the target molecules to pick-up the better activity. The detailed PLS data were shown in Table 5.

The linear relationship results shown in Fig. 6 between the activity *vs* predicted activity of the field and atom-based models had a worthy linear relationship. Besides, due to structural variations, a

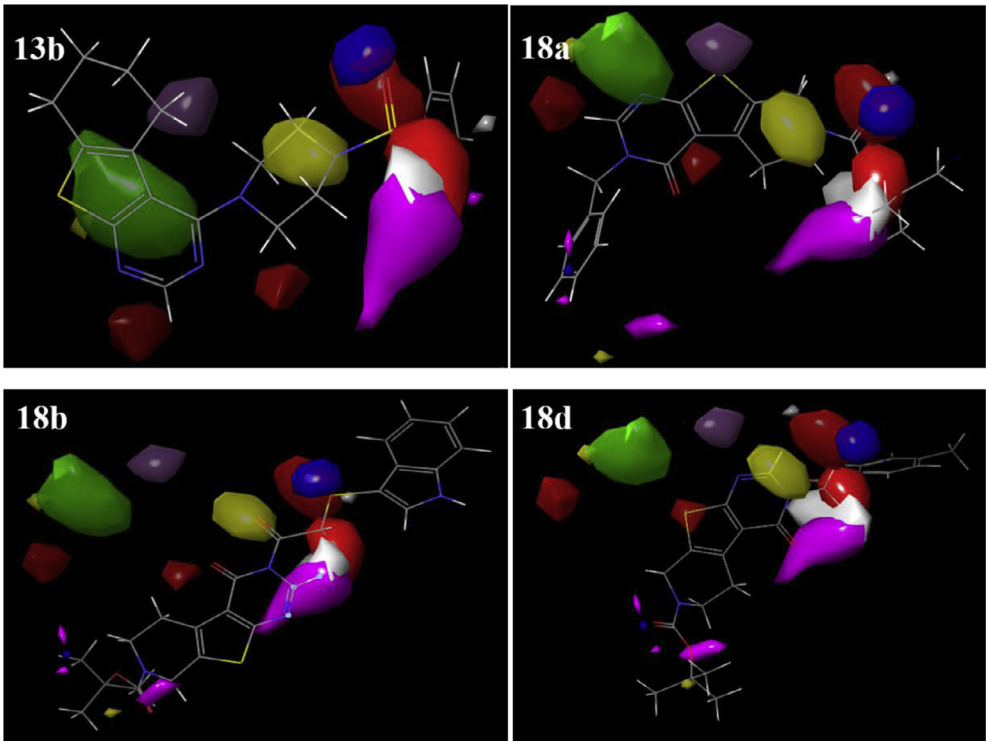

Fig. 7. Field-based contour maps of compound **13b, 18a, 18b** and **18d** (Field steric contours: the green contours indicate the areas that are conducive to steric interaction; Field electrostatic contours: the blue contours indicate the regions that are favourable to the positively charged groups, the red contours indicate the regions that are favourable to the negatively charged groups; Field hydrophobic contours: the yellow contours represent regions where hydrophobic groups increase activity, while the white contours highlight regions that would favour hydrophilic groups; Field hydrogen bond donor and acceptor contours: The magenta and the gray contours represent favourable and unfavourable hydrogen bond acceptor regions, respectively.).

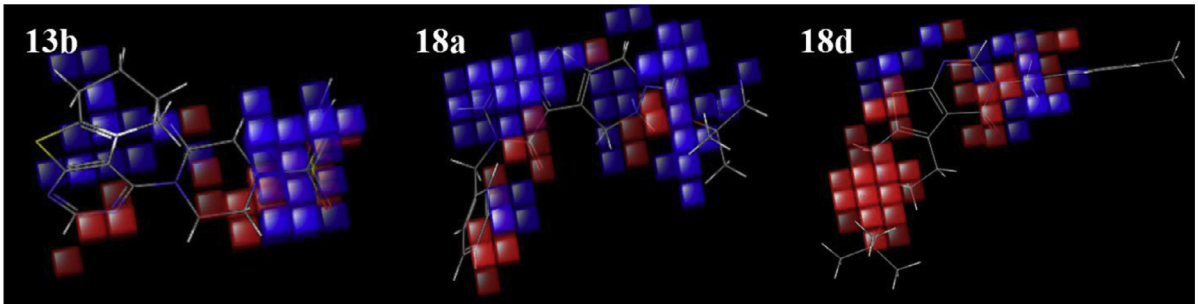

Fig. 8. Atom-based cubic maps of compound **13b, 18a** and **18d**. (Electron withdrawing contours: the pale red cubes indicate the areas that are conducive to favourable electron withdrawing interaction, Atom hydrophobic contours: the blue cubes represent regions where hydrophobic groups increase activity.

small amplitude instability was detected among the predicted activity values.

2.10. Contour analysis

In order to understand the impact of various fields on the target property, by Schrödinger software, Field and Atom contour maps were produced to recognise the impression of different fields (the steric field, electrostatic field, hydrophobic field and hydrogen bond donor and acceptor fields) on the activity data of compounds. StDev*Coeff mapping route was used to transform Field and atom-based models into visual results. All contour maps represented 80% level contributions for favoured and 20% level contributions for disfavoured. As indicated in Figs. 7 and Fig. 8, the template compounds **13b, 18a, 18b** and **18d** were chose to disclose the 3D-QSAR information of field and atom-based models. These results can support to understand the connection between structure and biological activity.

2.11. ADME/T properties

ADME/T properties of the synthesized compounds were calculated using Qikprop program (Qikprop, version 6.5, Schrödinger, LLC, New York, NY, 2014). As can be seen below, the partition coefficient (QPlogPo/w), hydrogen bond donors (donor HB), hydrogen bond acceptors (acceptor HB), molecular weight (mol. Wt.) and percent human oral absorption exhibited satisfactory results. The compounds also followed Lipinski rule of five. ADMET properties for Isoniazid and Rifampicin were also calculated and compared with the results of the synthesized compounds. The predicted results are shown in Table 6.

Table 6
ADME/T properties of active molecules.

Descriptors	Recommended values	13b	18a	18b	18c	18d	18e	18f	Levofloxacin	Isoniazid	Rifampicin
Molecular weight	130.0–725.0	448.98	397.49	442.48	466.38	439.52	475.56	476.59	361.37	137.141	820.978
Dipole moment	1.0–12.5	3.09	4.40	3.35	5.48	3.57	2.97	4.47	5.33	3.32	4.33
Total SASA	300–1000	669.54	699.24	737.81	719.49	773.04	809.35	821.15	587.16	329.909	1018.33
No. of rotatable bonds	0–15	2	3	4	3	4	4	4	1	2	25
Donor HB	0.0–6.0	0	0	0	0	0	0	1	0	3	6
Acceptor HB	2.0–20.0	7.0	6.5	7.5	6.5	8.5	7.0	7.0	7.25	4.5	20.35
QP Polarizability	13.0–70.0	43.25	44.63	46.46	45.30	47.32	50.81	51.26	36.38	13.80	68.019
QP logP o/w	2.0–6.5	3.856	4.201	3.412	4.877	3.726	3.807	5.095	-0.39	-0.653	2.893
QP log BB	−3.0 and 1.2	-0.178	-0.425	-1.513	-0.330	-0.898	-0.171	-0.849	-0.42	-0.87	-2.430
Human Oral Absorption	1–3	3	3	3	1	3	1	1	2	2	1
Percent Human Oral Absorption	> 80% is high	100	100	87.36	100	100	100	93.49	48.823	66.30	33.90
Rule of Five violations	< 25% is low	0	0	0	0	0	0	1	0	0	3

3. Conclusion

In conclusion, a library of 204 structurally diverse thienopyrimidines were designed and were subjected to preliminary *in silico* studies. 22 of the designed compounds were selected and synthesized based on their affinity towards TrmD and synthetic feasibility. The compounds were tested for their inhibitory activities against a panel of pathogens consisting *E. coli, S. aureus, K. pneuminiae, A. baumannii* and *P. aeruginosa* and *M. tuberculosis*. Among the tested compounds, **13b, 18a-e** were found to inhibit *M. tuberculosis* (ATCC 27294) with MIC of 16-32 µg/mL. The Compound **18f** exhibited selective and potent anti-bacterial activity with MIC value 4 µg/mL and was found to be nontoxic to Vero cells (CC_{50} = 50 µg/mL) with a good selectivity index (SI = >12.5). Further, 3D-QSAR and ADME/T studies were conducted to understand the mechanism of action and also physico chemical profile. Further exploration of the interesting potential TrmD inhibitors obtained will pave way for the development of new anti-microbial agents.

4. Experimental section

4.1. Materials and methods

Reactions were monitored by thin layer chromatography (TLC), which was performed on pre-coated TLC plates (Merck, TLC silica gel 60 F_{254}). Visualization of the spots on TLC plates was achieved either by UV light or by spraying with $KMnO_4$ or by phosphomolybdic acid stain solution or ninhydrin solution and heating the plates. All reactions were monitored by employing TLC technique using appropriate solvent system for development. All dry and air sensitive reactions were performed under Argon atmosphere with dry, freshly distilled solvents under anhydrous conditions. Dichloromethane was distilled freshly from P_2O_5. THF, dioxane and toluene was distilled over sodium-benzophenone. Yields reported are isolated yields of material. Commercial silica gel (200-400 mesh particle size, pH = 7) was used, wherever required. ^{1}H NMR spectra were recorded on Bruker Avance II 500 MHz instrument in DMSO or TFA. Chemical shifts are reported with respect to tetra methylsilane (Me_4Si) as the internal standard for ^{1}H NMR. The chemical shifts are expressed in parts per million (δ) downfield from Me_4Si. The standard abbreviations s, d, t, q, dd and m refer to singlet, doublet, triplet, quartet, double doublet and multiplet respectively. Coupling constant (J), whenever discernible, have been reported in Hz. Mass Spectra were recorded on Applied Biosystem MDS SCIEX model 4000-Q trap mass spectrometry using analyst 1.4.1 software.

Experimental procedure for the synthesis of *p*-amino salicylic acid linked thienopyrimidine derivatives:7, 9a-h:

To the mixture of cyclohexanone (**1**,1 mmol) and ethylcyanoacetate (**2**, 1 mmol) Sulphur powder (1 mmol) 10 ml of ethanol and TEA (1 mmol) was added and refluxed at 80-85 °C for 10-12 h, after the completion of reaction intermediate **3** is obtained to which 1.5 mmol of formamidine acetate and 5 ml of DMF was added and heated at 100 °C for 12 h to form the intermediate **4.** Then, intermediate **5** was obtained on chlorination of **4** (1 mmol) by thionyl chloride to which catalytic DMF was added and refluxed for 2-4 h. Equimolar amounts of intermediate **5** and *p*-amino salicylic acid (**6**,1 mmol) was taken and was added with 10 ml of 2-proponal and refluxed for 10-12 h. On cooling intermediate **7** was obtained which was treated with different arylsulphonylhalides in the presence of DIPEA (1 mmol), DCM at room temperature to acquire **9a-h** derivatives.

4.1.1. 2-hydroxy-4-((5,6,7,8-tetrahydrobenzo[4,5]thieno[2,3-d]pyrimidin-4-yl)amino)benzoic acid
(7)

Off-white solid; yield 80 %; mp:160–164 °C; FT-IR (cm−1): 3325, 3062, 1650, 1585, 780, 710; ^{1}H NMR (500 MHz, DMSO-d_6): δ 9.38 (s, 1H), 8.39 (s, 1H), 7.99 (s, 1H), 7.21 (dd, J = 10.0, 8.1 Hz, 1H), 7.17–7.08 (m, 1H), 7.05 (d, J = 8.0 Hz, 1H), 6.51 (dd, J = 7.9, 1.4 Hz, 1H), 3.12 (s, 2H), 2.82 (s, 2H), 1.85 (s, 4H); ^{13}C NMR (125 MHz, DMSO- d_6): δ 166.2, 158.0, 155.3, 152.5, 140.7, 133.4, 129.5, 127.1, 117.3, 113.0, 110.9, 109.4, 31.1, 25.8, 25.6, 22.6, 22.5; HRMS (ESI): *m/z* calculated for $C_{17}H_{15}N_3O_3S$ 342.1365 found 342.1393 $[M+H]^+$.

4.1.2. 2-((phenylsulfonyl)oxy)-4-((5,6,7,8-tetrahydrobenzo[4,5]thieno[2,3-d]pyrimidin-4-yl)amino)benzoic acid
(9a)

Off-white solid; yield 80 %; mp:160–164 °C; FT-IR (cm−1): 3325, 3062, 1650, 1585, 780, 710; ^{1}H NMR (500 MHz, DMSO-d_6): δ 8.38 (d, J = 10.6 Hz, 1H), 8.25 (s, 1H), 7.91 (t, J = 15.1 Hz, 2H), 7.83 (t, J = 7.4 Hz, 1H), 7.70 (t, J = 7.8 Hz, 2H), 7.63–7.47 (m, 2H), 7.40–7.26 (m, 1H), 6.71 (dd, J = 8.0, 1.7 Hz, 1H), 3.10 (s, 2H), 2.83 (s, 2H),

1.85 (s, 4H); ^{13}C NMR (125 MHz, DMSO- d_6): δ 166.6, 154.7, 152.2, 149.5, 141.3, 135.4, 135.1, 134.0, 130.3, 130.0, 128.7, 127.0, 120.6, 117.6, 116.5, 115.1, 25.7, 25.6, 22.6, 22.4; HRMS (ESI): *m/z* calculated for $C_{23}H_{19}N_3O_5S_2$ 482.0766 found 482.0787 $[M+H]^+$.

4.1.3. 2-(((4-chlorophenyl)sulfonyl)oxy)-4-((5,6,7,8-tetrahydrobenzo[4,5]thieno[2,3-d]pyrimidin-4-yl)amino)benzoic acid ***(9b)***

Off-white solid; yield 80 %; mp:160–164 °C; FT-IR (cm−1): 3325, 3062, 1650, 1585, 780, 710; ^{1}H NMR (500 MHz, DMSO-d_6): δ 8.37 (s, 1H), 8.26 (s, 1H), 7.92 (d, J = 8.6 Hz, 2H), 7.78 (d, J = 8.6 Hz, 2H), 7.56 (d, J = 8.0 Hz, 2H), 7.35 (t, J = 8.0 Hz, 1H), 6.79–6.73 (m, 1H), 3.10 (s, 2H), 2.84 (s, 2H), 1.85 (s, 4H);^{13}C NMR (125 MHz, DMSO- d_6): δ 166.6, 154.7, 152.2, 149.4, 141.3, 140.5, 134.1, 133.8, 130.7, 130.5, 130.2, 127.0, 120.7, 117.7, 116.6, 115.0, 25.7, 25.6, 22.6, 22.4; HRMS (ESI): *m/z* calculated for $C_{23}H_{18}ClN_3O_5S$ 516.0376 found 516.0398 $[M+H]^+$.

4.1.4. 2-(((2-chlorophenyl)sulfonyl)oxy)-4-((5,6,7,8-tetrahydrobenzo[4,5]thieno[2,3-d]pyrimidin-4-yl)amino)benzoic acid ***(9c)***

Off-white solid; yield 80 %; mp:160–164 °C; FT-IR (cm−1): 3325, 3062, 1650, 1585, 780, 710; ^{1}H NMR (500 MHz, DMSO-d_6): δ 8.37 (s, 1H), 8.28 (s, 1H), 7.97 (dd, J = 7.9, 1.6 Hz, 1H), 7.91 (dd, J = 8.0, 1.1 Hz, 1H), 7.82 (td, J = 7.8, 1.6 Hz, 1H), 7.71 (t, J = 2.2 Hz, 1H), 7.58 (td, J = 7.8, 1.2 Hz, 1H), 7.51 (dd, J = 8.2, 2.0 Hz, 1H), 7.35 (t, J = 8.2 Hz, 1H), 6.81 (ddd, J = 8.2, 2.4, 0.8 Hz, 1H), 3.10 (s, 2H), 2.84 (s, 2H), 1.85 (s, 4H); ^{13}C NMR (125 MHz, DMSO- d_6): δ 166.6, 154.6, 152.2, 149.3, 141.4, 136.9, 134.1, 133.0, 132.9, 132.8, 132.3, 130.2, 128.7, 127.0, 120.7, 117.7, 116.2, 114.6, 25.7, 25.6, 22.6, 22.4; HRMS (ESI): *m/z* calculated for $C_{23}H_{18}ClN_3O_5S_2$ 516.0376 found 516.0398 $[M+H]^+$.

4.1.5. 2-(((4-bromophenyl)sulfonyl)oxy)-4-((5,6,7,8-tetrahydrobenzo[4,5]thieno[2,3-d]pyrimidin-4-yl)amino)benzoic acid ***(9d)***

Off-white solid; yield 80 %; mp:160–164 °C; FT-IR (cm−1): 3325, 3062, 1650, 1585, 780, 710; ^{1}H NMR (500 MHz, DMSO-d_6): δ 8.37 (s, 1H), 8.27 (s, 1H), 7.93 (d, J = 8.6 Hz, 2H), 7.83 (d, J = 8.6 Hz, 2H), 7.56 (t, J = 5.2 Hz, 2H), 7.36 (t, J = 8.1 Hz, 1H), 6.76 (dd, J = 8.1, 1.5 Hz, 1H), 3.11 (s, 2H), 2.84 (s, 2H), 1.86 (s, 4H); ^{13}C NMR (125 MHz, DMSO- d_6): δ 166.6, 154.6, 152.2, 149.4, 141.3, 134.2, 134.1, 133.5, 130.7, 130.2, 129.8, 127.0, 120.7, 117.7, 116.6, 114.9, 25.7, 25.6, 22.6, 22.4; HRMS (ESI): *m/z* calculated for $C_{23}H_{18}BrN_3O_5S_2$ 561.0028 found 561.0016 $[M+2]^+$.

4.1.6. 2-(((4-(tert-butyl)phenyl)sulfonyl)oxy)-4-((5,6,7,8-tetrahydrobenzo[4,5]thieno[2,3-d]pyrimidin-4-yl)amino)benzoic acid ***(9e)***

Off-white solid; yield 80 %; mp:160–164 °C; FT-IR (cm−1): 3325, 3062, 1650, 1585, 780, 710; ^{1}H NMR (500 MHz, DMSO-d_6): δ 8.37 (s, 1H), 8.26 (s, 1H), 7.83 (d, J = 8.5 Hz, 2H), 7.69 (d, J = 8.5 Hz, 2H), 7.62–7.47 (m, 2H), 7.34 (t, J = 8.1 Hz, 1H), 6.79–6.71 (m, 1H), 3.10 (s, 2H), 2.83 (s, 2H), 1.85 (s, 4H), 1.27 (s, 8H); ^{13}C NMR (125 MHz, DMSO- d_6): δ 166.6, 158.7, 154.7, 152.2, 149.5, 141.3, 134.0, 132.2, 130.0, 128.6, 127.1, 127.0, 120.6, 117.6, 116.6, 115.1, 35.6, 31.0, 25.7, 25.6, 22.6, 22.4; HRMS (ESI): *m/z* calculated for $C_{27}H_{27}N_3O_5S_2$ 538.0681 found 538.0709 $[M+H]^+$.

4.1.7. 4-((5,6,7,8-tetrahydrobenzo[4,5]thieno[2,3-d]pyrimidin-4-yl)amino)-2-(tosyloxy)benzoic acid ***(9f)***

Off-white solid; yield 80 %; mp:156–159 °C; FT-IR (cm−1): 3325, 3062, 1650, 1585, 780, 710; ^{1}H NMR (500 MHz, DMSO-d_6): δ 8.38 (d, J = 10.6 Hz, 1H), 8.25 (s, 1H), 7.91 (t, J = 15.1 Hz, 2H), 7.83 (t, J = 7.4 Hz, 1H), 7.70 (t, J = 7.8 Hz, 2H), 7.63–7.47 (m, 1H), 7.40–7.26 (m, 1H), 6.71 (dd, J = 8.0, 1.7 Hz, 1H), 3.45 (s, 3H), 3.10 (s, 2H), 2.83 (s, 2H), 1.85 (s, 4H); HRMS (ESI): *m/z* calculated for $C_{24}H_{21}N_3O_5S_2$ 495.2048 found 495.2073 $[M+H]^+$.

4.1.8. 2-(((4-nitrophenyl)sulfonyl)oxy)-4-((5,6,7,8-tetrahydrobenzo[4,5]thieno[2,3-d]pyrimidin-4-yl)amino)benzoic acid ***(9g)***

Off-white solid; yield 80 %; mp:160–164 °C; FT-IR (cm−1): 3325, 3062, 1650, 1585, 780, 710; ^{1}H NMR (500 MHz, DMSO-d_6): δ 8.52–8.44 (m, 2H), 8.35 (s, 1H), 8.28 (s, 1H), 8.24–8.15 (m, 2H), 7.59 (d, J = 7.9 Hz, 2H), 7.36 (t, J = 8.1 Hz, 1H), 6.82–6.73 (m, 1H), 3.09 (s, 2H), 2.84 (s, 2H), 1.85 (s, 4H); ^{13}C NMR (125 MHz, DMSO- d_6): δ 166.6, 154.6, 152.2, 151.5, 149.2, 141.4, 140.2, 134.2, 130.6, 130.3, 127.0, 125.5, 120.9, 117.7, 116.5, 114.9, 25.6, 25.6, 22.6, 22.4; HRMS (ESI): *m/z* calculated for $C_{23}H_{18}N_4O_7S_2$ 527.0617 found 527.0640 $[M+H]^+$.

4.1.9. 2-(((2,4-dichlorophenyl)sulfonyl)oxy)-4-((5,6,7,8-tetrahydrobenzo[4,5]thieno[2,3-d]pyrimidin-4-yl)amino)benzoic acid ***(9h)***

Off-white solid; yield 80 %; mp:160–164 °C; FT-IR (cm−1): 3325, 3062, 1650, 1585, 780, 710; ^{1}H NMR (500 MHz, DMSO-d_6): δ 8.38 (s, 1H), 8.28 (s, 1H), 8.20 (d, J = 2.0 Hz, 1H), 7.94 (d, J = 8.6 Hz, 1H), 7.74–7.63 (m, 2H), 7.56–7.48 (m, 1H), 7.37 (t, J = 8.2 Hz, 1H), 6.85 (dd, J = 8.1, 1.9 Hz, 1H), 3.10 (s, 2H), 2.84 (s, 2H), 1.85 (s, 4H); ^{13}C NMR (125 MHz, DMSO- d_6): δ 166.6, 154.6, 152.1, 149.2, 141.5, 141.2, 134.2, 134.1, 133.7, 132.7, 131.8, 130.3, 128.9, 127.0, 120.8, 117.7, 116.3, 114.4, 25.6, 25.6, 22.6, 22.4; HRMS (ESI): *m/z* calculated for $C_{23}H_{17}Cl_2N_3O_5S_2$ 550.0065 found 550.0088 $[M+H]^+$.

Experimental procedure for the synthesis of piperazine linked thienopyrimidine derivatives: 13a-h

Equimolar amounts of intermediate **5** and piperazine (**10**,1mmol) was taken into RBF and add the quantity of 10 ml 2-proponal and refluxed for 10-12 h. On cooling intermediate **11** was obtained which was treated with different arylsulphonylchlorides (**12a-h**, 1 mmol) in the presence of DIPEA (1 mmol), DCM at room temperature to acquire **13a-h** derivatives.

4.1.10. 4-(4-(phenylsulfonyl)piperazin-1-yl)-5,6,7,8-tetrahydrobenzo[4,5]thieno[2,3-d] pyrimidine ***(13a)***

Off-white solid; yield 80 %; mp:160–164 °C; FT-IR (cm−1): 3325, 3062, 1650, 1585, 780, 710; ^{1}H NMR (500 MHz, Trifluoroacetic acid-*d*) δ 8.46 (s, 1H), 7.81 (dd, J = 19.6, 7.6 Hz, 2H), 7.77–7.69 (m, 1H), 7.64 (t, J = 7.8 Hz, 2H), 4.20 (s, 4H), 3.30 (d, J = 41.6 Hz, 4H), 3.03–2.91 (m, 2H), 2.85 (s, 2H), 2.11–2.00 (m, 2H), 1.84 (s, 2H); ^{13}C NMR (125 MHz, Trifluoroacetic acid-*d*) δ 160.1, 154.9, 143.6, 139.4, 134.9, 134.8, 133.7, 129.9, 129.9, 128.7, 127.5, 127.4, 118.8, 49.4, 46.0, 45.6, 28.0, 25.1, 22.2, 22.0; HRMS (ESI): *m/z* calculated $C_{20}H_{22}N_4O_2S_2$ 416.1561 for found 415.1590 $[M+H]^+$.

4.1.11. 4-(4-((2-chlorophenyl)sulfonyl)piperazin-1-yl)-5,6,7,8-tetrahydrobenzo[4,5]thieno[2,3-d]pyrimidine ***(13b)***

Off-white solid; yield 80 %; mp:160–164 °C; FT-IR (cm−1): 3325, 3062, 1650, 1585, 780, 710; ^{1}H NMR (500 MHz, Trifluoroacetic acid-*d*) δ 8.55 (s, 2H), 8.17 (d, J = 7.9 Hz, 2H), 7.68 (d, J = 3.4 Hz, 4H), 7.56 (dd, J = 4.7, 4.3 Hz, 2H), 4.39–4.13 (m, 11H), 3.63 (dd, J = 27.9, 23.2 Hz, 9H), 3.02 (t, J = 6.1 Hz, 5H), 2.93 (d, J = 17.0 Hz, 5H), 2.14–2.05 (m, 5H), 1.96–1.85 (m, 5H); ^{13}C NMR (125 MHz, Trifluoroacetic acid-*d*) δ 160.2, 154.9, 143.5, 139.4, 135.6, 133.8, 132.8, 132.5, 132.2, 128.7, 127.7, 118.9, 49.8, 45.5, 28.0, 25.0, 22.1, 21.9; HRMS (ESI): *m/z* calculated $C_{20}H_{21}ClN_4O_2S_2$ 449.0794 for found 449.0821 $[M+H]^+$.

4.1.12. 4-(4-((4-chlorophenyl)sulfonyl)piperazin-1-yl)-5,6,7,8-tetrahydrobenzo[4,5]thieno[2,3-d]pyrimidine
(13c)

Off-white solid; yield 80 %; mp:160–164 °C; FT-IR (cm−1): 3325, 3062, 1650, 1585, 780, 710; ^{1}H NMR (500 MHz, Trifluoroacetic acid-*d*) δ 8.48 (s, 1H), 7.76 (t, J = 9.1 Hz, 2H), 7.61 (d, J = 8.6 Hz, 2H), 4.22 (dd, J = 20.0, 15.8 Hz, 4H), 3.31 (d, J = 38.4 Hz, 4H), 3.04–2.91 (m, 2H), 2.85 (s, 2H), 2.05 (dd, J = 7.0, 3.6 Hz, 2H), 1.85 (d, J = 3.2 Hz, 2H); ^{13}C NMR (125 MHz, Trifluoroacetic acid-*d*) δ 160.1, 160.0, 154.9, 154.8, 143.6, 143.5, 142.3, 142.2, 139.5, 139.4, 132.4, 132.3, 130.3, 130.2, 128.8, 128.8, 128.7, 128.6, 118.8, 118.7, 49.3, 49.3, 45.9, 45.8, 28.0, 27.9, 25.0, 25.0, 22.1, 22.1, 21.9, 21.9; HRMS (ESI): *m/z* calculated $C_{20}H_{21}ClN_4O_2S_2$ 449.0794 for found 449.0821 $[M+H]^+$.

4.1.13. 4-(4-tosylpiperazin-1-yl)-5,6,7,8-tetrahydrobenzo[4,5]thieno[2,3-d]pyrimidine
(13d)

Off-white solid; yield 80 %; mp:160–164 °C; FT-IR (cm−1): 3325, 3062, 1650, 1585, 780, 710; ^{1}H NMR (500 MHz, Trifluoroacetic acid-*d*) δ 8.58 (s, 1H), 7.93–7.71 (m, 2H), 7.57 (d, J = 8.0 Hz, 2H), 4.35 (d, J = 34.7 Hz, 4H), 3.44 (s, 4H), 3.09 (t, J = 5.8 Hz, 2H), 2.97 (s, 2H), 2.58 (s, 3H), 2.17 (s, 2H), 1.96 (s, 2H); ^{13}C NMR (125 MHz, Trifluoroacetic acid-*d*) δ 160.0, 154.8, 147.1, 143.4, 139.3, 130.4, 128.6, 127.5, 118.6, 49.3, 45.9, 27.9, 25.0, 22.1, 21.9, 20.0; HRMS (ESI): *m/z* calculated for $C_{21}H_{24}N_4O_2S_2$ 429.2460 found 429.2488 $[M+H]^+$.

4.1.14. 4-(4-((4-bromophenyl)sulfonyl)piperazin-1-yl)-5,6,7,8-tetrahydrobenzo[4,5]thieno[2,3-d]pyrimidine
(13e)

Off-white solid; yield 80 %; mp:160–164 °C; FT-IR (cm−1): 3325, 3062, 1650, 1585, 780, 710; ^{1}H NMR (500 MHz, Trifluoroacetic acid-*d*) δ 8.72 (s, 3H), 8.08–7.99 (m, 7H), 7.92 (d, J = 8.6 Hz, 7H), 4.45 (s, 12H), 3.59 (s, 12H), 3.23 (t, J = 5.9 Hz, 7H), 3.10 (s, 6H), 2.30 (d, J = 5.5 Hz, 6H), 2.09 (s, 6H); ^{13}C NMR (125 MHz, Trifluoroacetic acid-*d*) δ 160.1, 154.8, 143.5, 139.4, 133.3, 133.1, 130.3, 128.8, 128.6, 118.8, 49.3, 45.8, 27.9, 25.0, 22.1, 21.9; HRMS (ESI): *m/z* calculated for $C_{20}H_{21}BrN_4O_2S_2$ 494.0289 found 494.0264 $[M+2]^+$.

4.1.15. 4-(4-((4-nitrophenyl)sulfonyl)piperazin-1-yl)-5,6,7,8-tetrahydrobenzo[4,5]thieno[2,3-d]pyrimidine
(13f)

Off-white solid; yield 80 %; mp:160–164 °C; FT-IR (cm−1): 3325, 3062, 1650, 1585, 780, 710; ^{1}H NMR (500 MHz, Trifluoroacetic acid-*d*) δ 8.79–8.75 (m, 1H), 8.34 (d, J = 8.5 Hz, 1H), 5.55–5.47 (m, 1H), 4.52 (d, J = 21.6 Hz, 2H), 3.68 (s, 2H), 3.23 (d, J = 30.9 Hz, 1H), 3.13 (s, 1H), 2.33 (s, 1H), 2.12 (s, 1H); ^{13}C NMR (125 MHz, Trifluoroacetic acid-*d*) δ 160.2, 154.9, 151.1, 143.6, 141.4, 139.6, 129.0, 128.6, 125.1, 119.0, 52.5, 49.4, 45.9, 27.9, 25.1, 22.1, 21.9; HRMS (ESI): *m/z* calculated for $C_{20}H_{21}N_5O_4S_2$ 460.1035 found 460.1069 $[M+H]^+$.

4.1.16. 4-(4-((2,4-dichlorophenyl)sulfonyl)piperazin-1-yl)-5,6,7,8-tetrahydrobenzo[4,5]thieno[2,3-d]pyrimidine
(13g)

Off-white solid; yield 80 %; mp:160–164 °C; FT-IR (cm−1): 3325, 3062, 1650, 1585, 780, 710; ^{1}H NMR (500 MHz, Trifluoroacetic acid-*d*) δ 8.75 (s, 1H), 8.28 (t, J = 10.3 Hz, 1H), 7.88 (d, J = 1.7 Hz, 1H), 7.73 (dd, J = 8.6, 1.7 Hz, 1H), 4.41 (s, 4H), 3.85 (s, 4H), 3.22 (s, 2H), 3.11 (s, 2H), 2.29 (s, 2H), 2.09 (s, 2H); ^{13}C NMR (125 MHz, Trifluoroacetic acid-*d*) δ 160.0, 154.8, 143.5, 142.2, 139.4, 132.3, 130.2, 128.8, 128.6, 118.8, 49.3, 45.8, 45.4, 27.9, 25.0, 22.1, 21.9; HRMS (ESI): *m/z* calculated $C_{20}H_{20}Cl_2N_4O_2S_2$ 483.0405 for found 483.0440 $[M+H]^+$.

4.1.17. 4-(4-((4-(tert-butyl)phenyl)sulfonyl)piperazin-1-yl)-5,6,7,8-tetrahydrobenzo[4,5]thieno[2,3-d]pyrimidine
(13h)

Off-white solid; yield 80 %; mp:160–164 °C; FT-IR (cm−1): 3325, 3062, 1650, 1585, 780, 710; ^{1}H NMR (500 MHz, Trifluoroacetic acid-*d*) δ 8.47 (s, 2H), 7.73 (dd, J = 23.3, 8.7 Hz, 9H), 4.20 (s, 8H), 3.35 (s, 8H), 2.97 (t, J = 6.0 Hz, 4H), 2.85 (s, 4H), 2.05 (dd, J = 7.1, 3.5 Hz, 4H), 1.84 (d, J = 3.2 Hz, 4H), 1.37 (s, 18H); ^{13}C NMR (125 MHz, Trifluoroacetic acid-*d*) δ 160.2, 160.0, 154.8, 143.5, 139.3, 130.4, 128.7, 127.4, 127.1, 118.7, 49.3, 45.9, 35.1, 29.7, 28.0, 25.0, 22.2, 21.9; HRMS (ESI): *m/z* calculated $C_{24}H_{30}N_4O_2S_2$ 474.1312 for found 474.1359 $[M+H]^+$.

Experimental procedure for the synthesis of linked *N*-Boctetrahydropyrido thienopyrimidine derivatives:

To the starting material tert-butyl4-oxopiperidine-1-carboxylate (**14**, 1 mmol) ethylcyano acetate (**2**, 1 mmol), Sulphur powder (1 mmol), 10 mL of ethanol and TEA (1 mmol) was added and refluxed for 10-12 h, after the completion of reaction intermediate **15** was obtained to which formamidine acetate (1.5 mmol) and 10 mL of DMF was added and heated at 100 °C for 12 h to procure intermediate **16**. Then, intermediate **16** was treated with equimolar amounts of aryl halides (**17a-f**), K_2CO_3 which was used as base and 5 mL of DMF and the reaction for carried at room temperature for 12 h. After cooling aryl substituted *N*-Boc tetrahydropyrido thienopyrimidine analogues **18a-f** were obtained.

4.1.18. Tert-butyl3-benzyl-4-oxo-3,5,6,8-tetrahydropyrido[4′,3′:4,5]thieno[2,3-d]pyrimidine-7(4H)-carboxylate
(18a)

Off-white solid; yield 80 %; mp:160–164 °C; FT-IR (cm−1): 3325, 3062, 1650, 1585, 780, 710; ^{1}H NMR (500 MHz, DMSO-d_6): δ 8.58 (s, 1H), 7.40–7.28 (m, 5H), 5.18 (s, 2H), 4.59 (s, 2H), 3.61 (t, J = 5.1 Hz, 2H), 2.93 (s, 2H), 1.43 (s, 9H); ^{13}C NMR (125 MHz, DMSO-d_6): δ 162.8, 157.2, 154.4, 148.5, 137.2, 130.1, 129.1, 128.1, 121.9, 79.8, 48.9, 28.5, 26.0; HRMS (ESI): *m/z* calculated for $C_{21}H_{23}N_3O_3S$ 396.0846 found 398.0879 $[M+H]^+$.

4.1.19. Tert-butyl3-(3-nitrobenzyl)-4-oxo-3,5,6,8-tetrahydropyrido[4′,3′:4,5]thieno[2,3-d]pyrimidine-7(4H) -carboxylate
(18b)

Off-white solid; yield 80 %; mp:160–164 °C; FT-IR (cm−1): 3325, 3062, 1650, 1585, 780, 710; ^{1}H NMR (500 MHz, DMSO-d_6): δ 8.67 (s, 1H), 8.27 (s, 1H), 8.16 (dd, J = 8.2, 1.4 Hz, 1H), 7.82 (d, J = 7.7 Hz, 1H), 7.69–7.62 (m, 1H), 5.31 (s, 2H), 4.59 (s, 2H), 3.61 (t, J = 5.6 Hz, 2H), 2.92 (t, J = 5.6 Hz, 2H), 1.43 (d, J = 6.7 Hz, 9H); ^{13}C NMR (125 MHz, DMSO-d_6): δ 163.0, 157.3, 154.4, 148.4, 139.2, 135.1, 130.6, 130.1, 123.3, 123.1, 122.0, 79.9, 48.6, 28.5, 25.9; HRMS (ESI): *m/z* calculated for $C_{21}H_{22}N_4O_5S$ 443.1494 found 443.1520 $[M+H]^+$.

4.1.20. Tert-butyl 3-(2,6-dichlorobenzyl)-4-oxo-3,5,6,8-tetrahydropyrido[4′,3′:4,5]thieno[2,3-d]pyrimidine-7(4H)-carboxylate
(18c)

Off-white solid; yield 80 %; mp:160–164 °C; FT-IR (cm−1): 3325, 3062, 1650, 1585, 780, 710; ^{1}H NMR (500 MHz, DMSO-d_6): δ 8.26 (s, 1H), 7.52 (d, J = 8.2 Hz, 2H), 7.41 (dd, J = 8.7, 7.5 Hz, 1H), 5.39 (d, J = 11.6 Hz, 2H), 4.58 (s, 2H), 3.59 (t, J = 5.6 Hz, 2H), 2.89 (t, J = 5.6 Hz, 2H), 1.42 (s, 9H); ^{13}C NMR (125 MHz, DMSO-d_6): δ 162.5, 157.1, 154.4, 148.3, 136.2, 131.3, 131.0, 130.1, 129.5, 121.8, 79.9, 46.4, 28.5, 25.9; HRMS (ESI): *m/z* calculated for $C_{21}H_{21}Cl_2N_3O_3S$ 466.0681 found 466.0708 $[M+H]^+$.

4.1.21. Tert-butyl 4-oxo-3-(2-oxo-2-(p-tolyl)ethyl)-3,5,6,8-tetrahydropyrido[4′,3′:4,5] thieno [2,3-d]pyrimidine-7(4H)-carboxylate ***(18d)***

Off-white solid; yield 80 %; mp:160–164 °C; FT-IR (cm−1): 3325, 3062, 1650, 1585, 780, 710; ^{1}H NMR (500 MHz, DMSO-d_6): δ

8.34 (s, 1H), 7.99 (d, J = 8.2 Hz, 2H), 7.43 (d, J = 8.0 Hz, 2H), 5.59 (d, J = 11.2 Hz, 2H), 4.60 (d, J = 17.5 Hz, 2H), 3.63 (t, J = 5.6 Hz, 2H), 2.92 (t, J = 5.6 Hz, 2H), 2.43 (s, 3H), 1.44 (d, J = 7.4 Hz, 9H); ^{13}C NMR (125 MHz, DMSO-d_6): δ 192.6, 163.1, 157.2, 154.4, 148.9, 145.2, 132.4, 130.0, 128.6, 121.7, 79.9, 52.0, 28.5, 25.9, 21.7; HRMS (ESI): *m/z* calculated for $C_{23}H_{25}N_3O_4S$ 440.1566 found 440.1592 $[M+H]^+$.

4.1.22. Tert-butyl 3-(2-(naphthalen-2-yl)-2-oxoethyl)-4-oxo-3,5,6,8-tetrahydropyrido[4′,3′:4,5] thieno[2,3-d]pyrimidine-7(4H)-carboxylate ***(18e)***

Off-white solid; yield 80 %; mp:160–164 °C; FT-IR (cm−1): 3325, 3062, 1650, 1585, 780, 710; ^{1}H NMR (500 MHz, DMSO-d_6): δ 8.89 (s, 1H), 8.40 (s, 1H), 8.25–7.98 (m, 4H), 7.71 (dt, J = 14.6, 7.0 Hz, 2H), 5.77 (s, 2H), 4.61 (d, J = 20.3 Hz, 2H), 3.63 (s, 2H), 2.93 (s, 2H), 1.42 (d, J = 20.6 Hz, 9H); ^{13}C NMR (125 MHz, DMSO-d_6): δ 193.1, 163.1, 157.2, 154.4, 148.9, 135.9, 132.6, 132.2, 132.1, 130.8, 130.2, 130.1, 129.6, 129.2, 128.3, 127.7, 123.7, 121.7, 79.9, 52.2, 28.5, 25.9; HRMS (ESI): *m/z* calculated for $C_{26}H_{25}N_3O_4S$ 477.3609 found 477.3644 $[M+H]^+$.

4.1.23. Tert-butyl 3-(2-((1H-indol-3-yl)thio)acetyl)-4-oxo-3,5,6,8-tetrahydropyrido[4′,3′:4,5]thieno[2,3-d]pyrimidine-7(4H)-carboxylate ***(18f)***

White solid; yield 82 %; mp:150–153 °C; FT-IR (cm−1): 3325, 3062, 1650, 1585, 780, 710; ^{1}H NMR (500 MHz, DMSO-d_6): δ 8.58 (s, 1H), 7.40–7.28 (m, 5H), 5.18 (s, 2H), 4.59 (s, 2H), 3.61 (t, J = 5.1 Hz, 2H), 2.93 (s, 2H), 1.43 (s, 9H); ^{13}C NMR (125 MHz, DMSO-d_6): δ 163.0, 157.3, 154.4, 148.4, 139.2, 135.1, 130.6, 130.1, 123.3, 123.1, 122.0, 79.9, 48.6, 43.3, 28.5, 25.9; HRMS (ESI): *m/z* calculated for $C_{24}H_{24}N_4O_4S_2$ 498.1108 found 498.1133 $[M+H]^+$.

4.2. Bacterial strains and media

The panel of bacteria consisted of *Escherichia coli* (ATCC 25922), *Klebsiella pneumoniae* (BAA-1705), *Acinetobacter baumannii* (BAA1605), *Pseudomonas aeruginosa* (ATCC 27853) and *Staphylococcus aureus* (ATCC 29213). NRS199, NRS129, NRS186, NRS191, NRS192, NRS193, NRS194, NRS198 are MRSA strains while VRS1, VRS4, VRS12 are VRSA strains. These strains were obtained from BEI/NARSA/ATCC (Biodefense and Emerging Infections Research Resources Repository/Network on Antimicrobial Resistance in *Staphylococcus aureus*/American Type Culture Collection, USA) and routinely cultivated on Mueller-Hinton Agar (MHA). Prior to the experiment, a single colony was picked from MHA plate, inoculated in Mueller-Hinton cation supplemented broth II (CA-MHB) and incubated overnight at 37 °C with shaking for 18–24 h to get the starter culture.

M. tuberculosis H37Rv ATCC 27294 was cultured in Middlebrook 7H9 (Difco, Becton, NJ, USA) media supplemented with 10% ADC (Bovine Serum Albumin, Dextrose, NaCl), 0.2% glycerol and 0.05% Tween-80 (ADC-Tween-80).

4.2.1. Antibiotic susceptibility testing against pathogen panel

Antibiotic susceptibility testing was carried out on the newly synthesized compounds by determining the Minimum Inhibitory Concentration (MIC) with reference to the standard CLSI guidelines [17,18]. MIC is defined as the minimum concentration of compound at which visible bacterial growth is inhibited. Bacterial cultures were grown in Mueller-Hinton cation supplemented broth (CA-MHB). Optical density (OD_{600}) of the cultures was measured, followed by dilution for ~10^6 cfu/mL. This inoculum was added into a series of test wells in a microtitre plate that contained various concentrations of compound under test ranging from 64-4 μg/mL. Controls i.e., cells alone and media alone (without compound+cells) and levofloxacin used as a reference standard. Plates were incubated at 37 °C for 16-18 h followed by observations of MIC values by the absence or presence of visible growth. For each compound, MIC determinations were performed independently thrice using duplicate samples each time.

4.2.2. Antibiotic susceptibility testing against pathogenic mycobacteria

Antimycobacterial susceptibility testing was carried out on the newly synthesized compounds by using broth micro dilution assay [19]. 1g/100 mL stock solutions of test and control compounds were prepared in DMSO and stored in −20 °C. Mycobacterial cultures were inoculated in Middlebrook 7H9 enriched (Difco, Becton, NJ, USA) media supplemented with 10% ADC-Tween-80 (Bovine Serum Albumin, Dextrose, 0.2% glycerol and 0.05% Tween-80) and OD_{600} of the cultures was measured, followed by dilution to achieve ~10^6 cfu/mL [20]. The newly synthesized compounds were tested from 0.0064–0.00005 g/100 mL in two-fold serial diluted fashion with 2.5 μL of each concentration added per well of a 96-well round bottom micro titre plate. Later, 97.5 μL of bacterial suspension was added to each well containing the test compound along with appropriate controls. Presto blue (Thermo Fisher, USA) resazurin-based dye was used for the visualized identification of active compounds. MIC of active compound was determined as lowest concentration of compound that inhibited visible growth after incubation period. For each compound, MIC determinations were replicated thrice using duplicate samples. The MIC plates were incubated at 37 °C for 7 days for Mtb.

4.3. Molecular docking

The molecular docking studies were performed at the binding site of TrmD (PDB ID: 1UAK) [5]. The coordinates of the crystal structure were obtained from RCSB-Protein Data Bank and suitable corrections were made using Protein Preparation Wizard from the Schrödinger package. Regarding the ligands, molecules were constructed using ChemBio3D Ultra 12.0 and their geometries were optimized using molecular mechanics. Finally, docking studies were performed according to the standard protocol implemented in maestro software, version 9.9 on the most active molecules [21]. The ligand-protein complex was analysed for interactions and 3D pose of most active compounds was imaged using Schrödinger. In this work, in order to further investigate the anti-bacterial activity of target compounds against TrmD, the in vitro activity data was chose to construct the 3D-Quantitative Structure Activity Relationship (3D-QSAR) models. Field and atom-based analysis were performed using MIC values for all target compounds against antibacterial activity. Construction of all target compounds, structural optimization, and 3D-QSAR modelling were all performed on maestro software, version 9.9 [22].

Authorship statement

All persons who meet authorship criteria are listed as authors, and all authors certify that they have participated sufficiently in the work to take public responsibility for the content, including participation in the concept, design, analysis, writing, or revision of the manuscript. Furthermore, each author certifies that this material or similar material has not been and will not be submitted to or published in any other publication before its appearance in the *Journal of Molecular Structure*.

Declaration of Competing Interest

The authors declare no conflicts of interest.

Acknowledgements

S. M is thankful to Department of Pharmaceuticals, Ministry of Chemicals & Fertilizers, Govt. of India, for the award of NIPER fellowship. This study was supported by the DST grant from Department of Science and Technology, Govt. of India to S.N and S.C. (EMR/2017/000220), NIPER Communication no: NIPER-H/2020/M115.

References

[1] P.A. Elkins, J.M. Watts, M. Zalacain, A. Van Thiel, P.R. Vitazka, M. Redlak, C. Andraos-Selim, F. Rastinejad, W.M. Holmes, Insights into catalysis by a knotted TrmD tRNA methyltransferase, J. Mol. Biol. 333 (2003) 931–949.

[2] H.J. Ahn, H.W. Kim, H.J. Yoon, B.I. Lee, S.W. Suh, J.K. Yang, Crystal structure of tRNA (m1G37) methyltransferase: insights into tRNA recognition, EMBO J. 22 (2003) 2593–2603.

[3] K. O'Dwyer, J.M. Watts, S. Biswas, J. Ambrad, M. Barber, H. Brule, C. Petit, D.J. Holmes, M. Zalacain, W.M. Holmes, Characterization of *Streptococcus pneumoniae* TrmD, a tRNA methyltransferase essential for growth, J. Bacteriol. 186 (2004) 2346–2354.

[4] S. Goto-Ito, T. Ito, M. Kuratani, Y. Bessho, S. Yokoyama, Tertiary structure checkpoint at anticodon loop modification in tRNA functional maturation, Nat. Struct. Mol. Biol. 16 (2009) 1109–1115.

[5] [(a)] P.J. Hill, A. Abibi, R. Albert, B. Andrews, M.M. Gagnon, N. Gao, T. Grebe, L.I. Hajec, J. Huang, S. Livchak, S.D. Lahiri, D.C. McKinney, J. Thresher, H. Wang, N. Olivier, E.T. Buurman, Selective inhibitors of bacterial t–RNA-(N1G37) methyltransferase (TrmD) that demonstrate novel ordering of the lid domain, J. Med. Chem. 56 (2013) 7278–7288; [(b)] W. Zhong, K.K. Pasunooti, S. Balamkundu, Y.H. Wong, Q. Nah, V. Gadi, S. Gnanakalai, Y.H. Chionh, M.E. McBee, P. Gopal, S.H. Lim, N. Olivier, E.T. Buurman, T. Dick, C.F. Liu, J. Lescar, P.C. Dedon, Thienopyrimidinone derivatives that inhibit bacterial tRNA (Guanine37–N^1)–methyl transferase (TrmD) by restructuring the active site with a tyrosine-flipping mechanism, J. Med. Chem. 62 (2019) 7788–7805.

[6] A.J. Whitehouse, S.E. Thomas, K.P. Brown, A. Fanourakis, D.S.H. Chan, M.D.J. Libardo, V. Mendes, H.I.M. Boshoff, R.A. Floto, C. Abell, T.L. Blundell, A.G. Coyne, Development of inhibitors against *Mycobacterium abscessus* tRNA (m1G37) methyltransferase (TrmD) using fragment-based approaches, J. Med. Chem. 62 (2019) 7210–7232.

[7] W. Zhong, A. Koay, A. Ngo, Y. Li, Q. Nah, Y.H. Wong, Y.H. Chionh, H.Q. Ng, X. Koh-Stenta, A. Poulsen, K. Foo, M. McBee, M.L. Choong, A. El Sahili, C. Kang, A. Matter, J. Lescar, J. Hill, P. Dedon, Targeting the bacterial epitranscriptome for antibiotic development: discovery of novel tRNA-(N1G37) methyltransferase (TrmD) inhibitors, ACS Infect. Dis. 5 (2019) 326–335.

[8] [(a)] A.E. Amr, A.M. Mohamed, S.F. Mohamed, N.A. Abdel-Hafez, A.G. Hammam, Anticancer activities of some newly synthesized pyridine, pyrane, and pyrimidine derivatives, Bioorg. Med. Chem. 14 (2006) 5481–5488; [(b)] T. Horiuchi, J. Chiba, K. Uoto, T. Soga, Discovery of novel thieno[2,3-d]pyrimidin-4-yl hydrazone-based inhibitors of Cyclin D1-CDK4: synthesis, biological evaluation, and structure–activity relationships, Bioorg. Med. Chem. Lett. 19 (2009) 305–308.

[9] (a) M.A. Elsherbeny, M.B. Elashmawy, H.I. Elsubbagh, A.A. Elemam, F.A. Badria, Synthesis, antimicrobial and antiviral evaluation of certain thienopyrimidine derivatives, Eur. J. Med. Chem. 30 (1995) 445–449; (b) B.V. Ashalatha, B. Narayana, K.K.V. Raj, N.S. Kumari, Synthesis of some new bioactive 3-amino-2-mercapto-5,6,7,8-tetrahydro[1]benzothieno[2,3-d]pyrimidin-4(3H)-one derivatives, Eur. J. Med. Chem. 42 (2007) 719–728; (c) A.E. Rashad, A.H. Shamroukh, R.E. Abdel-Megeid, W.A. El-Sayed, Synthesis, reactions, and antimicrobial evaluation of some polycondensed thienopyrimidine derivatives, Synth. Commun. 40 (2010) 1149–1160; (d) R.V. Chambhare, B.G. Khadse, A.S. Bobde, R.H. Bahekar, Synthesis and preliminary evaluation of some N-[5-(2-furanyl)-2-methyl-4-oxo-4H-thieno[2,3-d]pyrimidin-3-yl]-carboxamide and 3-substituted-5-(2-furanyl)-2-methyl-3H-thieno[2,3-d]pyrimidin-4-ones as antimicrobial agents, Eur. J. Med. Chem. 38 (2003) 89–100.

[10] A.E. Rashad, A.H. Shamroukh, R.E. Abdel-Megeid, A. Mostafa, R. El-Sheshteny, A. Kandeil, M.A. Ali, K. Banert, Synthesis and screening of some novel fused thiophene and thienopyrimidine derivatives for anti-avian influenza virus (H5N1) activity, Eur. J. Med. Chem. 45 (2010) 5251–5257.

[11] V. Alagarsamy, S. Meena, K.V. Ramseshu, V.R. Solomon, K. Thirumurugan, K. Dhanabal, M. Murugan, Synthesis, analgesic, anti-inflammatory, ulcerogenic index and antibacterial activities of novel 2-methylthio-3-substituted-5,6,7,8-tetrahydrobenzo(b)thieno[2,3-d]pyrimidin-4(3H)-ones, Eur. J. Med. Chem. 41 (2006) 1293–1300.

[12] J.F. Deng, L. Peng, G.C. Zhang, X.B. Lan, C.F. Li, F.X. Chen, Y.Y. Zhou, Z.X. Lin, L. Chen, R.K. Dai, H.J. Xu, L. Yang, X.Q. Zhang, W.H. Hu, The highly potent and selective dipeptidyl peptidase IV inhibitors bearing a thienopyrimidine scaffold effectively treat type 2 diabetes, Eur. J. Med. Chem. 46 (2011) 71–76.

[13] Y. Kotaiah, N. Harikrishna, K. Nagaraju, C.V. Rao, Eur. J. Med. Chem. 58 (2012) 340–345 A.E.E. Amr, M.H. Sherif, M.G. Assy, M.A. Al-Omar, I. Ragab, Antiarrhythmic, serotonin antagonist and antianxiety activities of novel substituted thiophene derivatives synthesized from 2-amino-4,5,6,7-tetrahydro-N-phenylbenzo[b]thiophene-3-carboxamide, Eur. J. Med. Chem. 45 (2010) 5935-5942.

[14] H.N. Hafez, H.A.R. Hussein, A.R.B.A. Gazzar, Synthesis of substituted thieno[2,3-d]pyrimidine-2,4-dithiones and their S-glycoside analogues as potential antiviral and antibacterial agents, Eur. J. Med. Chem. 45 (2010) 4026–4034.

[15] S.E. Abbas, N.M.A. Gawad, R.F. George, Y.A. Akar, Synthesis, antitumor and antibacterial activities of some novel tetrahydrobenzo[4,5]thieno[2,3-d]pyrimidine derivatives, Eur. J. Med. Chem. 65 (2013) 195–204.

[16] S.G. Li, C. Vilcheze, S. Chakraborty, X. Wang, H. Kim, M. Anisetti, S. Ekins, K.Y. Rhee, W.R. Jacobs, J.S. Freundlich, Evolution of a thienopyrimidine antitubercular relying on medicinal chemistry and metabolomics insights, Tetrahedron Lett. 56 (2015) 3246–3250.

[17] P.A. Wayne, Methods for dilution antimicrobial susceptibility tests for bacteria that grow aerobically, approved standard, CLSI document M07-A9 Ninth ed., Clinical and Laboratory Standards Institute, 2012.

[18] J.H. Jorgensen, J.F. Hindler, L.B. Reller, M.P. Weinstein, New consensus guidelines from the clinical and laboratory standards institute for antimicrobial susceptibility testing of infrequently isolated or fastidious bacteria, Clin. Infect. Dis. 44 (2007) 280–286.

[19] [(a)] M. Pandey, A.K. Singh, R. Thakare, S. Talwar, P. Karaulia, A. Dasgupta, S. Chopra, A.K. Pandey, Diphenyleneiodonium chloride (DPIC) displays broad-spectrum bactericidal activity, Sci. Rep. 7 (2017) 11521; [(b)] I. Wiegand, K. Hilpert, R.E. Hancock, Agar and broth dilution methods to determine the minimal inhibitory concentration (MIC) of antimicrobial substances, Nat. Protoc. 3 (2008) 163–175.

[20] B. Rivas-Santiago, C.E.R. Santiago, J.E. Castañeda-Delgado, J.C. León–Contreras, R.E. Hancock, R. Hernandez-Pando, Activity of LL-37, CRAMP and antimicrobial peptide-derived compounds E2, E6 and CP26 against *M. tuberculosis*, Int. J. Antimicrob. Agents 41 (2013) 143–148.

[21] Y. Zhang, Y. Chen, D. Zhang, L. Wang, T. Lu, Y. Jiao, Discovery of novel potent VEGFR–2 inhibitors exerting significant antiproliferative activity against cancer cell lines, J. Med. Chem. 61 (2018) 140–157.

[22] R. Cao, X. Guan, B. Shi, Z. Chen, Z. Ren, W. Peng, H. Song, Design, synthesis and 3D-QSAR of β-carboline derivatives as potent antitumor agents, Eur. J. Med. Chem. 45 (2010) 2503–2515.